Impact of Concrete Building Structures on Neutron Radiation and its Mitigation

Svenja Sonder, Simon Hebel, Carina Prünte, Gerald Kirchner

Carl-Friedrich von Weizsäcker-Zentrum für Naturwissenschaft und Friedensforschung, Universität Hamburg, Beim Schlump 83, 20144 Hamburg
E-mail: svenja.sonder@uni-hamburg.de

Abstract:

A key technique for nuclear disarmament verification is neutron counting. Such measurements take place in nuclear facilities with concrete rooms. Neutron scattering in building structures can create a significant background, leading to higher measured neutron flux densities as well as a moderated energy distribution. Since neutron measurements may become a major tool in nuclear disarmament verification, assessing the influence of concrete is important for this application. Using Monte Carlo simulations, the impact of concrete building structures on the neutron radiation has been analysed for different scenarios. For a single wall it is shown that for energies between 1 eV and 14 MeV the ratio between reflected and transmitted neutrons depends on the source energy. Moreover, scattering in the concrete causes thermalisation of the neutron energy spectrum. Exchanging regular Portland concrete with radiation protection concrete leads to less reflected and transmitted neutrons, but in the MeV range the difference between the concrete types is small. In a closed room, neutron flux densities depend on the thickness of the walls, the room size, and the concrete composition. In a small room flux densities may be nearly an order of magnitude higher than in an open environment. Different concrete compositions can alter flux densities by a factor of 2 and significantly impact their energy spectra. The effect of the walls can be mitigated by enclosing both measurement sample and detector in a standardised neutron absorbent casing.

Keywords: nuclear disarmament; neutron counting; concrete; neutron scattering

1. Introduction

Despite a reduction of nuclear weapons stockpiles in the past decades, there is still no verification regime enforcing the global irreversible disarmament of nuclear warheads. Since 2015, the International Partnership for Nuclear Disarmament Verification (IPNDV) is developing verification approaches, procedures, and technologies [1].

Disarmament verification procedures include gamma and neutron radiation measurements to confirm the presence or absence of fissile material as well as spectrometric analyses to validate its isotopic composition [2, 3]. The specific measurement techniques (active or passive, count rate or spectrometry) are still under discussion, but it is widely assumed they will include passive neutron counting. In using a method called template measurement a container holding a nuclear warhead can be measured at various different stages of the dismantlement process to ensure its contents have remained unchanged [4] without revealing absolute or relative values of properties that characterize the item. However, if the measurements conducted in different environments were to yield different results for the same item, the template method would falsely indicate the diversion or manipulation of fissile material.

In closed rooms, concrete walls influence measurements by absorbing, moderating, and reflecting neutrons. Corrections for neutron scattering from walls etc. are not readily available but methods were developed e.g. for the calibration of neutron detectors [5]. As the exact shielding characteristics of concrete are highly important for radiation protection, they are widely studied, e.g. for radioactive waste [6] or for spallation sources for which a special concrete with polyethylene and boron carbide has been developed to effectively shield the neutron radiation [7]. Differences in shielding effectiveness [8] and their effect on reactivities of fissile materials [9-11] have been analysed for different concrete compositions, but there is a lack of assessments of their reflection potential.

Neutron reflection by concrete is important in the verification of nuclear disarmament since the reflected neutrons can reach a detector and increase the measured neutron flux. Gregor et al. [12] have shown how the neutron signal of a detector in a closed room deviates from the simplified $1/d^2$ assumption and that this deviation depends on the measurement environment. They concluded that at distances of practical interest greater than 50 cm from the neutron source, the reflected neutrons outnumber the direct neutrons and therefore the calculation of the source activity based on the measured neutron flux densities has to be corrected for this effect. They also demonstrated experimentally the effect of room sizes on measurement results. Analytic expressions [13] as well as Monte Carlo

simulations [14] have shown that for small and intermediate sized rooms reflected neutron flux densities correlate well with room surface areas.

In disarmament verification, measurements on an intact warhead are assumed to take place at a distance of at least 1 m from the warhead [15]. Therefore, the effect of walls on the measured neutron flux densities, which is significant as discussed above, has to be taken into account.

In this paper, a systematic analysis of the impact of concrete building structures on neutron radiation will be presented based on Monte Carlo simulations of neutron transport. It includes a neutron beam directed at a single wall as well as neutron flux densities of an intact warhead modelled after the Fetter design [16] in a closed concrete room. The impact of the concrete composition is analysed for ordinary concrete as well as radiation protection concrete. The thickness of the building structures in nuclear weapons facilities may be unknown or undisclosed. Therefore, a series of simulations were performed varying the thickness of the concrete structures. Finally, the effect of room size was analysed.

2. Materials and Methods

In this study, Monte Carlo simulations were performed, as these allow varying concrete composition, density, and changes in its hydrogen concentration due to varying humidity [10]. Gregor et al. have shown that Monte Carlo simulation can well reproduce neutron measurements in concrete rooms [12]. We used the open-source simulation toolkit Geant4, which has been developed at CERN, the European Organization for Nuclear Research, and is used in various applications including high energy physics as well as medical science [17]. The ENDF/B-VIII.0 cross section library [18] was used. Fission processes were simulated with the G4ParticleHPFission model. The applicability of our code has been validated using plutonium-uranium mixed oxide configurations of various masses, shieldings (bare, cadmium, lead, high-density polyethylene), and concentrations as well as isotopic compositions of the plutonium [19].

Ordinary concrete like Portland concrete and radiation protection concrete with additives such as boron and barium were investigated. A range of concrete compositions are specified in Table 1.

The thickness of walls in nuclear facilities is generally not disclosed for security reasons. A value of 20 cm was chosen as a reasonable default wall thickness which was then systematically varied to quantify the effect on the simulated neutron scattering.

Element	Mass fraction [%]		
	Portland	**Baryte**	**Boron carbide**
Hydrogen	1.00	0.36	0.36
Boron	–	–	61.55
Carbon	0.10	–	17.16
Oxygen	52.91	31.16	9.58
Fluorine	–	–	–
Sodium	1.60	–	–
Magnesium	0.20	0.12	0.12
Aluminium	3.39	0.42	0.42
Silicon	33.70	1.05	1.05
Sulphur	–	10.79	–
Potassium	1.30	–	–
Calcium	4.40	5.02	5.02
Manganese	–	–	–
Iron	1.40	4.75	4.75
Zinc	–	–	–
Barium	–	46.34	–
Density [g/cm³]	2.30	3.35	2.30

Table 1: Composition of the different types of concrete. The Portland and Baryte concrete specifications are taken from McConn Jr. et al. [20], the Boron carbide concrete composition is the authors' own estimate whereby the structural properties have not been checked to be suitable for walls. Nevertheless, it gives a good impression of the effect of a high boron amount in concrete.

As neutron source for our calculations, the notional warhead model developed by Fetter et al. [16] was adopted. It consists of a hollow sphere of 4 kg of weapon-grade plutonium surrounded by a beryllium reflector, an uranium tamper, high explosives (such as triaminotrinitrobenzene [21]) and an aluminium casing. For security and safety reasons, the warhead is placed in a steel container with a Celotex lining (Fig. 1), a lignocellulosic fibreboard whose chemical composition can be approximated by cellulose [20]. The plutonium has a primary neutron source strength of approximately 190 kBq due to spontaneous fission of Pu-240. The energy distribution of the neutrons emitted by the plutonium was modelled as a Watt spectrum

$$X(E) = exp\left(\frac{-E}{a}\right) \cdot sinh\left(\sqrt{b \cdot E}\right)$$

with the Watt parameters a = 0.7949 MeV and b = 4.689 MeV-1 [22].

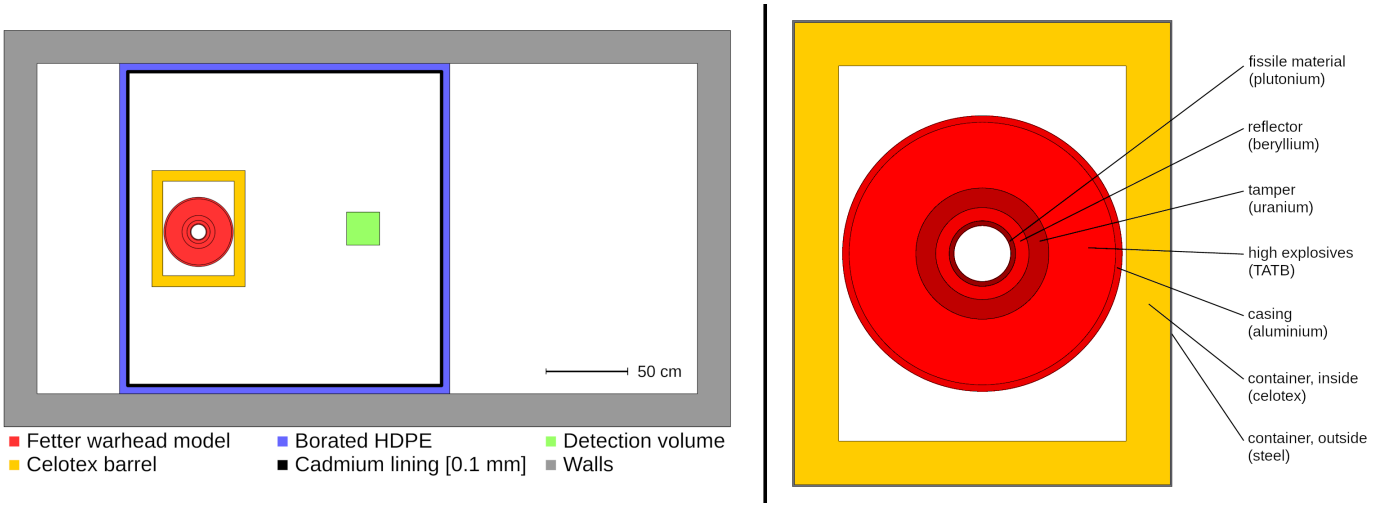

Figure 1: Side view cut (left) of the simulated standard geometry. A nuclear warhead, as modelled by Fetter [16], (right) is placed in a Celotex container in a 4 m by 3 m by 2 m room. Neutron flux densities are counted in the detection volume. For the simulation presented in Section 4, a 2 m by 2 m by 2 m neutron shielding box containing borated high-density polyethylene was placed around source and detection volume in order to mitigate neutron back scattering from the walls.

Two scenarios were studied: I. A neutron beam directed at a concrete wall and II. A nuclear warhead positioned in a closed room with concrete walls.

Scenario I:

To systematically study the impact of concrete walls on neutrons, a beam directed at a single wall was simulated. A monoenergetic point source was emitting neutrons towards the centre of a 4 m by 4 m concrete wall. In the simulation, neutron energies were varied between 1 eV and 14 MeV. Reflected as well as transmitted neutrons were counted, and their energy spectra recorded.

In addition, the effect of reinforced concrete was studied by assuming a lattice of 2 cm diameter high carbon steel [20] bars present at the centre of the wall. They were placed at 10 cm intervals in both directions.

Scenario II:

During nuclear dismantlement verification inspections, measurements will presumably be performed in closed rooms. The background will include not only neutrons scattered back from air, walls, floor and ceiling, but also neutrons eventually entering the detector after multiple scattering events in the room structure. A simplified scenario of such a measurement setup has been analysed.

A reference room with a floor area of 4 m by 3 m and a height of 2 m was modelled. Its floor, ceiling and walls are assumed to consist of 20 cm thick Portland concrete. A notional nuclear warhead with a primary neutron activity by spontaneous fission of Pu-240 of 190 kBq (secondary neutrons are produced by induced fission in Pu with a neutron activity of 360 kBq and by neutron interaction processes in the reflector and tamper of 162 kBq) according to Fetter et al. [16] is situated in a steel container with a 6.6 cm thick Celotex lining. The container is placed 1 m away from the centre of the room. The warhead model has a radius of 21 cm, its container a radius of 28.5 cm and a height of 71 cm.

The room geometry was varied by successively shifting the walls outward in steps of 1 m, thereby enlarging the room from 4 m by 3 m to 24 m by 23 m. For each size, simulations were repeated for three different heights of the ceiling (2, 4 and 6 m).

Instead of simulating a specific detector, the neutron flux densities in a 20 cm by 20 cm by 20 cm sampling volume made of air located at the centre of the room were simulated and recorded. Positioning the detector 1 m from the warhead container is a reasonable assumption for an inspection [15].

3. Results and discussion

3.1 Neutron beam directed at a single wall

The fractions of neutrons which are reflected, absorbed, or transmitted by a 20 cm wall of the concrete types studied are given in Figure 2. Some general trends become apparent. First, there are only slight differences between Portland and Baryte concrete despite their different composition. In contrast, neutrons with source energies of 1 MeV and lower show high absorption rates in boron carbide concrete. This effect becomes more pronounced for lower source energies, which closely reflects the energy dependence of the boron absorption cross section. Second, for neutrons with source energies typical for a fission spectrum (exceeding 1 MeV) the reflected fraction decreases about 50 % compared to source energies of 1 MeV or lower for all three

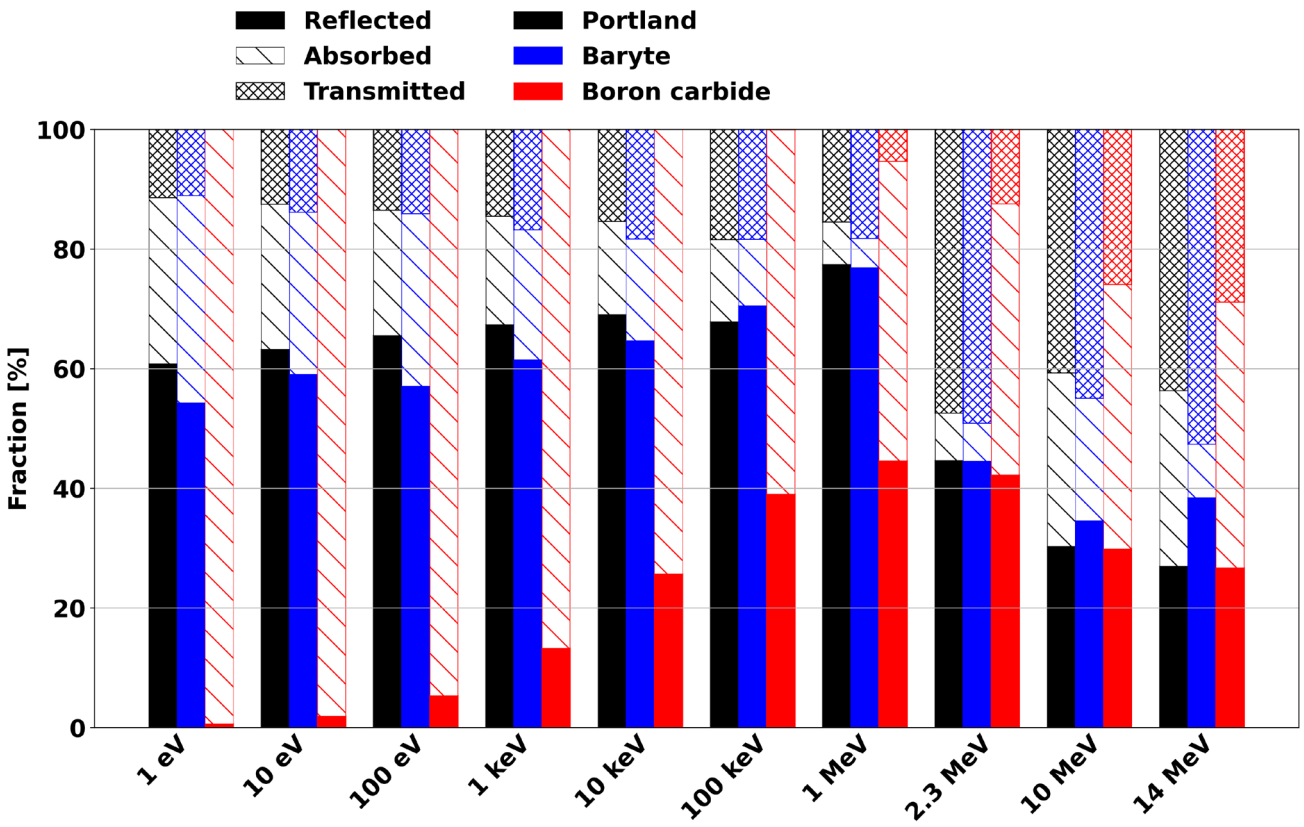

Figure 2: Fractions of reflected, transmitted and absorbed neutrons for a 20 cm concrete wall, by source energy and concrete type.

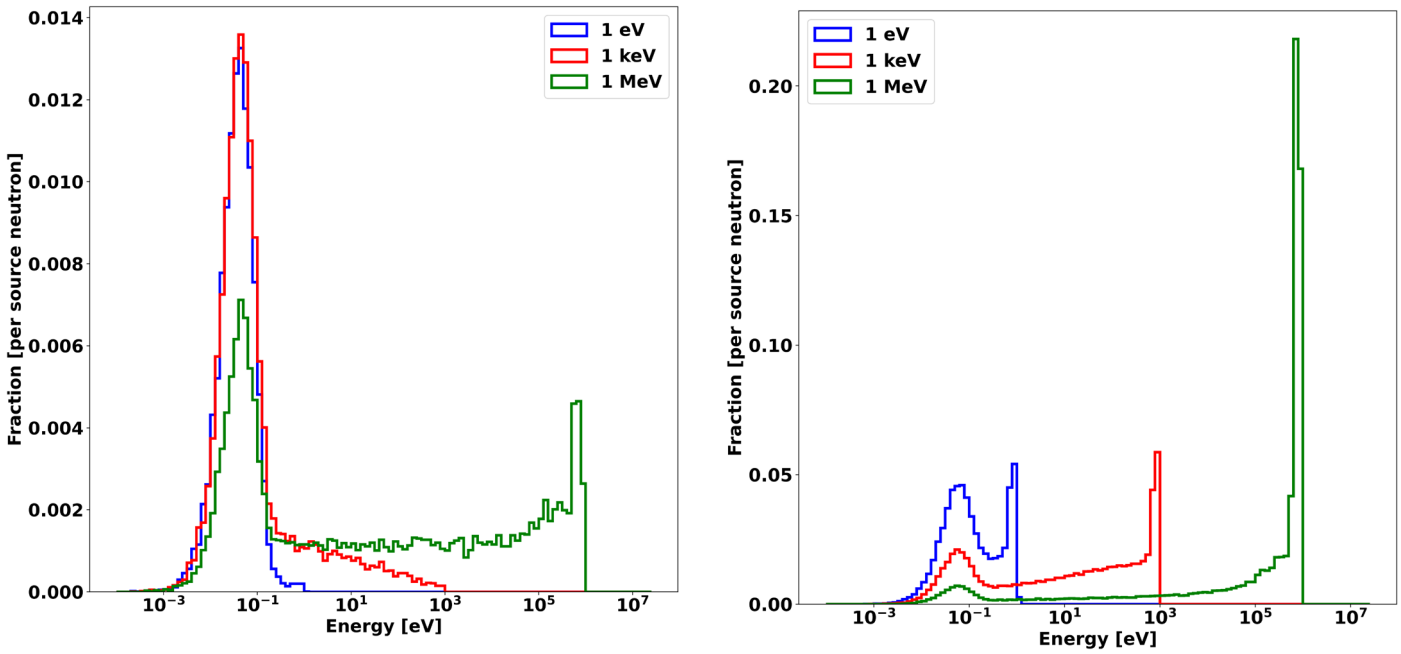

Figure 3: Energy distributions of transmitted (left) and reflected (right) neutrons by a Portland concrete wall for three different source energies.

concrete types. Again, the boron carbide concrete shows an elevated absorption rate due to neutron moderation within the concrete and absorption by ^{10}B.

If reinforced with steel rebar (results not shown), the fractions of reflected neutrons are slightly higher for all three concrete types (< 5 %). The transmitted fractions are slightly affected by additional absorptions of moderated neutrons by the steel.

These results confirm and extend previous analyses on the reflection of neutrons by concrete building structures [8, 12-14]. This reflection is even present if building structures consist of boron carbide concrete intended for effective neutron shielding, although neutron background levels are considerably reduced compared to ordinary Portland or high-density gamma shielding Baryte concrete

For the common Portland concrete, energy spectra of reflected and transmitted neutrons are shown in Figure 3 for three different source energies. For the transmitted neutrons (Fig. 3, left), the moderating effect of the concrete becomes obvious: at source energies of 1 eV and 1 keV transmitted neutrons are almost thermalised, but even 44% of the transmitted 1 MeV neutrons display energies < 1 eV after transmission. The energy distributions of the reflected neutrons (Fig. 3, right) demonstrate the small scattering cross section of fast neutrons compared to epithermal and thermal source energies.

The reinforced concretes (results not shown) do not show significantly different energy distributions of reflected neutrons, but a slightly smaller thermal peak of transmitted neutrons due to the higher absorption of low energy neutrons in the steel. Since the presence of rebar does not have a major impact and information on the design of the concrete structures in nuclear weapons handling facilities is expected to be confidential, the results presented in the following are for pure concretes.

3.2 Nuclear warhead in a closed room

In the following, the flux densities and energy distributions of neutrons emitted from the notional warhead model entering the detection volume in the closed concrete room are analysed. Results are shown in Table 2 and Fig. 4 for room structures with concrete walls of 20 cm thickness. For comparison, results are included for the hypothetical case that no surrounding structures are present to indicate the direct neutron flux. For the common Portland, but also for Baryte concrete, reflected neutrons dominate flux densities at the detection volume, but even for the neutron shielding B_4C concrete reflected neutrons contribute about 33% to the recorded signal. As was shown in Fig. 3 above, both Portland and Baryte concrete effectively moderate the reflected neutrons. Differences in peak heights at thermal energies are caused by the higher hydrogen content of the Portland concrete (compare Table 1). Thermalisation is not visible for boron carbide concrete structures due to the strong absorption of scattered neutrons with energies below 100 eV. Fig. 4 shows that even without any background of reflected neutrons, the emitted spectrum is moderated. This effect is caused by the high explosives of the warhead.

concrete type	flux density [cm^{-2} s^{-1}]	flux density in absorption box [cm^{-2} s^{-1}]
none	2.14 ± 0.03	3.20 ± 0.04
Portland	5.71 ± 0.05	3.25 ± 0.04
Baryte	4.82 ± 0.05	3.32 ± 0.04
Boron carbide	2.84 ± 0.04	3.26 ± 0.04

Table 2: Neutron flux densities in the detection volume for different concrete types of the building materials. The second column shows the flux densities when source and detection volume are enclosed in a neutron absorbent box made from borated polyethylene and cadmium.

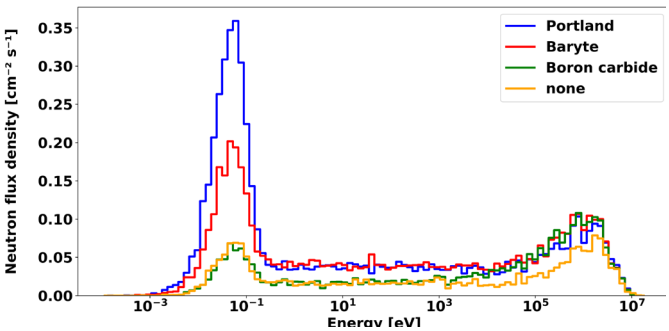

Figure 4: Energy distributions of neutrons inside the detection volume in the reference concrete room for various types of concrete; for comparison, a spectrum without any reflecting structures outside the nuclear warhead is shown.

3.3 Thickness of building structures

The simulation results shown in Fig. 5 show that due to reflection in the Portland concrete neutron flux densities in the room rise quickly when increasing the thickness of the walls (including floor and ceiling), converging already at approximately 20 cm. The physical reason for this convergence is the penetration depth of the reflected neutrons (Fig. 6): the vast majority of the reflected neutrons do not penetrate the concrete more than 15–20 cm. Since it is reasonable to assume that walls in nuclear weapon maintenance and storage facilities commonly will exceed this value, the simulations presented here for a default thickness of 20 cm can be generalized.

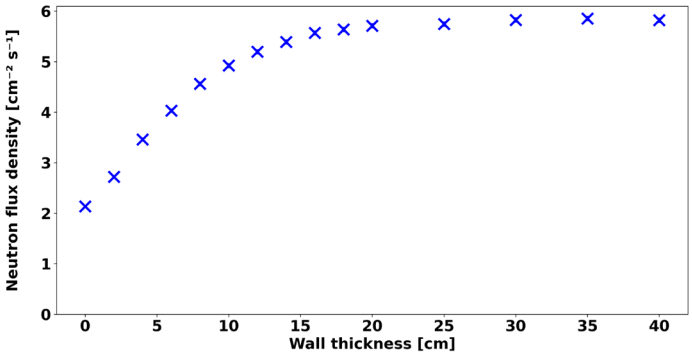

Figure 5: Calculated neutron flux densities in the detection volume as a function of building structure thickness for the notional Fetter nuclear warhead model.

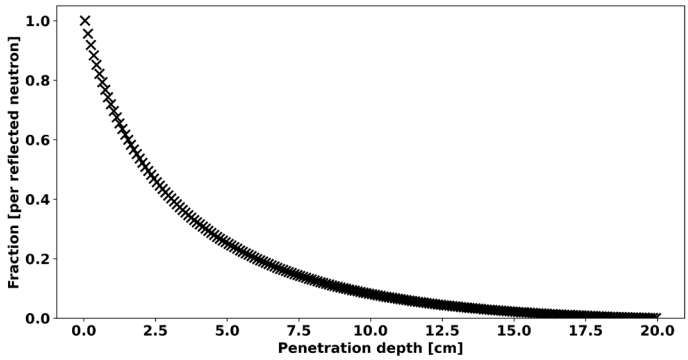

Figure 6: Penetration depth of neutrons before they are reflected back into the reference room. Each bin shows the cumulative fraction of neutrons reaching the designated depth. Absorbed and transmitted neutrons are not counted.

3.4 Room size

Simulated neutron flux densities within the modelled detector volume for varying room sizes are shown in Fig. 7. The value without any surrounding structures is given as reference. When enlarging the room area, the calculated neutron flux densities become smaller until they converge when the wall shift reaches 4 m, corresponding to a room size of 12 m by 11 m. At this point, the converged flux density is still larger than without concrete building structures as the floor is still present. A corresponding effect is observed when increasing height of the room until the neutron flux converges at about 4 m. However, for all room sizes the contribution of scattered neutrons to the total flux density remains significant and a small room may increase it by a factor of 2 compared to a large room.

4. Mitigating the impact of concrete structures

Due to the high price of boron carbide concrete, which is around 3300 times that of Portland concrete [23], routine operations (nuclear warhead maintenance, dismantlement, storage, and verification measurements) will most likely be performed in ordinary concrete buildings with high neutron reflection potential. For nuclear disarmament verification promising analytical technologies include neutron template

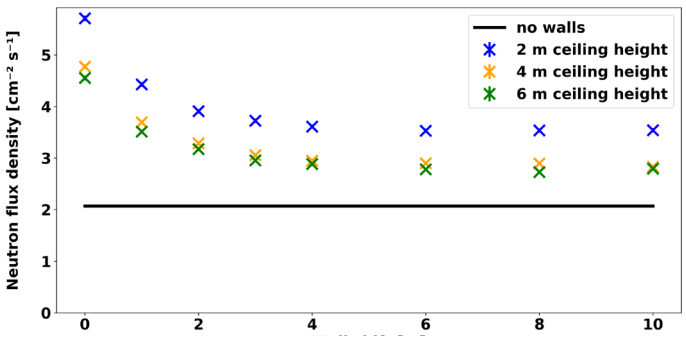

Figure 7: Neutron flux densities for the notional nuclear warhead in the modelled detector volume as a function of room area and ceiling height. The simulated room size starts out at 3 m by 4 m and is successively increased by shifting all walls outward. The straight line shows the flux density without any reflected neutrons.

measurements [4] and imaging [24]. Depending on the concrete and on the position of source and detector relative to the building walls reflected neutrons may dominate the neutron signals and invalidate such analyses.

Thus, a strategy to mitigate the influence of concrete structures on measured neutron signals is proposed. Inspired by the Pulsed Neutron Interrogation Test Facility (PUNITA) at the Joint Research Center of the European Commission [25], it is suggested to place sample and detector inside a box, which is designed (i) to minimise neutron flux densities leaving the box and therefore backscattering and, (ii) to reduce reflected neutron fluxes before entering the box' interior. This is achieved by using materials with high neutron moderation and absorption potentials [26]. In the following the effect of a cubic box of 2 m by 2 m by 2 m is analysed, which allows keeping a suitable distance between warhead container and detector. Walls, bottom and top of the container are made from 5 cm borated (35 %) high-density polyethylene slabs. An inner lining of 0.01 cm cadmium foil is included to absorb thermal neutrons and minimise backscattering of moderated neutrons into the detector volume. It was confirmed (data not shown) that increasing the thickness of the polyethylene shields did not have a significant effect on the neutrons flux inside the box.

The simulation results in Table 2 show that when using this measurement box, the recorded neutron flux densities are nearly identical for all concrete types and even for the hypothetical scenario that no neutron reflecting material is present outside the box. Comparison with the corresponding flux densities without the shielding box indicate that about 30% of the neutrons reaching the detector volume are backscattered by the polyethylene box itself. As expected, this results in shifting the energy distribution of the neutrons in the detector volume to lower energies, but without masking the spectrum of the neutrons emitted by the warhead (Fig. 8).

These results demonstrate that by using a shielding box as described the influence of concrete building structures on the neutron flux densities can be eliminated while keeping its own moderating effect of the neutrons at a tolerable level.

Using such boxes hence allows to apply almost all neutron verification technologies at each position during the nuclear disarmament process (deployment area, interim and long-term storage, dismantlement facility) without being affected by concrete walls, although their sizes may need to be adjusted for some measurement technologies. A significant neutron activation of their materials is not to be expected, since the materials of the proposed box are identical with those of neutron coincidence counters used in safeguards. It can be expected that each facility used for this process will have some area which will be dedicated to verification activities including potential gamma and neutron measurements. Each of these could be provided with such a shielding box for neutron verification analyses under standardised conditions. These may include template measurements – both of total fluxes and of energy distributions with e.g. a Bonner sphere type detector [27] for verification of the presence of high explosives in an assembled warhead – as well as imaging analyses [24]. Since the number of dismantlement facilities will be limited in each nuclear weapon state, the effort for installing the boxes will be low despite their weight and lack of mobility.

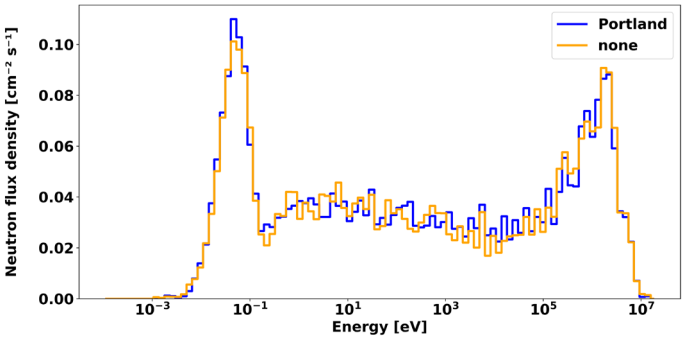

Figure 8: Spectra of the neutrons inside the sampling volume when neutron source and sampling volume are situated within a neutron absorption box consisting of polyethylene and cadmium.

5. Conclusions

The results presented in this study contribute to the knowledge on flux densities and energy distributions of neutrons reflected and transmitted by concrete building structures. These effects are quantified as functions of concrete types, including a highly borated concrete, room size and thickness of the concrete structures.

For its application in the context of nuclear disarmament verification, neutron measurement results should ideally be independent of sample positioning and the surrounding building structures, in particular for neutron imaging and template measurements, which rely on the reproducibility of neutron flux densities and their energy distributions. This problem can be solved by conducting the measurement in a neutron absorbent casing, constructed from borated polyethylene and an inner cadmium liner. Calculations show that such a casing has the potential to mitigate the influence of neutron reflection from the surrounding walls while introducing only a moderate and reproducible background of neutrons backscattered by the casing. Installing such a box in those facilities of the nuclear weapons complex which will be dedicated to disarmament verification activities will contribute to flexible and versatile nuclear disarmament verification strategies and to the confidence they will achieve.

6. References

[1] Hinderstein C; International Partnership for Nuclear Disarmament Verification: Laying a foundation for future arms reductions; Bulletin of Atomic Scientist; vol. 74; 2018; pp. 305-311; see also https://www.ipndv.org, accessed August 2022.

[2] Runkle RC, Bernstein A, Vanier PE; Securing special nuclear material: Recent advances in neutron detection and their role in nonproliferation; Journal of Applied Physics; vol. 108; 2010; 111101.

[3] Göttsche M, Kirchner G; Measurement Techniques for Warhead Authentication with Attributes: Advantages and Limitations; Science & Global Security; vol. 22; 2014; pp. 83-110.

[4] Yan J, Glaser A; Nuclear Warhead Verification: A Review of Attribute and Template Systems; Science & Global Security; vol. 23; 2015; pp. 157-170.

[5] Kim SI et al.; A review of neutron scattering correction for the calibration of neutron survey meters using the shadow cone method; Nuclear Engineering and Technology; vol. 47; 2015; pp. 939-944.

[6] Jallu F, Passard C, Brackx E; Application of active and passive neutron nondestructive assay methods to concrete radioactive waste drums; Nuclear Instruments and Methods in Physics Research B; vol. 269; no. 18; 2011; pp. 1956-1962.

[7] DiJulio DD et al; A polyethylene-B4C based concrete for enhanced neutron shielding at neutron research facilities; Nuclear Instruments and Methods in Physics Research A; vol. 859; 2017; pp. 41-46.

[8] Piotrowski T; Neutron shielding evaluation of concretes and mortars: A review; Construction and Building Materials; vol. 277; 2021; 122238.

[9] Handley GR, Robinson RC, Cline JC; Effects of Concrete Composition in Nuclear Criticality Calculations; Transactions of the American Nuclear Society; vol. 61; 1880; pp. 182-184.

[10] Wetzel LL; Amount and Effect of Moisture Retention in Concrete; Data Analysis for Nuclear Criticality Safety; vol. 63; 1991; pp.217-218.

[11] Monahan SP; The Neutron Physics of Concrete Reflectors; Fifth International Conference on Nuclear Criticality Safety; Albuquerque; 17 – 21 September 1995; LA-UR-95-2196; Revised; LA-UR-07-5898; 2007; https://mcnp.lanl.gov/pdf_files/la-ur-07-5898.pdf (accessed October 12, 2022).

[12] Gregor J, Baron M, Kesten J, Kroeger EA; Comparision of the response of handheld neutron detectors in differing deployment environments: Measurements, calculations and practical implications; Radiation Measurements; vol. 143; 2021; 106571.

[13] Eisenhauer CM, Hunt JB, Schwarz RB; Calibration Techniques of Neutron Personal Dosimetry; Radiation Protection Dosimetry; vol. 10; 1985; pp. 43-57.

[14] Khabaz R; Analysis of neutron scattering components inside a room with concrete walls; Applied Radiation and Isotopes; vol. 95; 2015; pp. 1-7.

[15] Oral communication by representatives of nuclear weapon states during IPNDV meetings.

[16] Fetter S et al.; Detecting Nuclear Warheads; Science & Global Security; vol. 1; 1990; pp. 225-263.

[17] Allison J et al.; Geant4 developments and applications; IEEE Transactions on Nuclear Science; vol. 53; 2006; pp. 270-278.

[18] Brown DA et al.; ENDF/B-VIII.0: The 8th Major Release of the Nuclear Reaction Data Library with CIELO-project Cross Sections, New Standards and Thermal Scattering Data; Nuclear Data Sheets; vol. 148; February 2018; pp. 1-142.

[19] Kreutle M, Borella A, Rossa R, Scholten C, Kirchner G, van der Meer C; Benchmarking Monte Carlo Simulations in the context of nuclear disarmament verification via Monte Carlo simulations with GEANT4; INMM & ESARDA Joint Virtual Annual Meeting; 23. - 26. 8. & 30. 8. - 1. 9. 2021.

[20] McConn Jr. RJ, Gesh CJ, Pagh RT, Rucker RA, Williams III RG; Compendium of Material Composition Data for Radiation Transport Modelling; Pacific West Laboratory; 2011.

[21] Withworth NJ; Modelling detonation in ultrafine TATB hemispherical boosters using CREST; Conference “Shock Compression of Condensed Matter – 2011”; Chicago; 26 June – 1 July 2011; American Institute of Physics Conference Proceedings 1426 (2012); pp. 213-216.

[22] Shores E; Data updates for the SOURCES-4A computer code; Nuclear Instruments and Methods in Physics Research B; vol. 179; no. 2; 2001; pp. 78-82.

[23] Federal German Association of the Cement Industry; Heavy Concrete / Radiation Protection Concrete; Cement Data Sheet Concrete Technology B 10; 2002 (in German).

[24] Brennan J et al.; Demonstration of two-dimensional time-encoded imaging of fast neutrons; Nuclear Instruments and Methods in Physics Research A; vol. 802; 2015; pp. 76-81.

[25] Favalli A, Mehner H-C, Crochemore, J-M, Pedersen B; Pulsed Neutron Facility for Research in Illicit Trafficing and Nuclear Safeguards; IEEE Transactions on Nuclear Science; vol. 56; 2009; pp. 1292-1296.

[26] Stone MB; Crow L; Fanelli VR; Niedziela JL; Characterization of shielding materials used in neutron scattering instrumentation; Nuclear Instruments and Methods in Physics Research A; vol. 946; 2019; 162708.

[27] Dubeau J, Hakmana Witharana SS, Atanackovic J, Yonkeu A, Archambault JP; A Neutron Spectrometer Using Nested Moderators; Radiation Protection Dosimetry; vol. 150; 2012; pp. 217-222.